

Plastic solar cells with engineered interfaces

Xugang Guo^{a,b} and Tobin J. Marks^a

^a Department of Chemistry, the Materials Research Center, and the Argonne-Northwestern Solar Energy Research Center, Northwestern University, 2145 Sheridan Road, Evanston, Illinois 60208, USA

^b Department of Chemistry, South University of Science and Technology of China, No. 1088, Xueyuan Blvd, Shenzhen, Guangdong, 518055, China

ABSTRACT

We discuss here bulk-heterojunction polymer solar cells with engineered interfaces to achieve desired phase separations (vertical and horizontal), molecule orientations, ohmic contacts, and electronic properties for device performance maximization, and to enhance the device durability by eliminating corrosive interfacial layers. The strategies discussed include development of novel interfacial layers such as self-assembled organic layers and inorganic metal oxide layers, and using inverted cell architectures. Interface engineering leads to optimal active layer morphologies and to polymer π -orientation, as well as maximum open circuit voltage. Using p-type NiO as the anode hole transporting/electron blocking layer results in dramatically enhanced device performance of P3HT/PCBM polymer solar cells with PCEs up to 5%. Electrical property and surface morphology investigations of NiO elucidate the mechanism for the enhanced performance. Other novel interfacial materials such as self-assembled organic monolayers and graphene oxide (GO) have also been incorporated into polymer solar cells to achieve comparable PCEs with improved device stability. Using ZnO as electron transporting/hole blocking layer and employing an inverted device architecture, polymer solar cells achieve desired molecule π -orientation and vertical phase separation, therefore extremely high fill factors and promising power conversion efficiencies. In addition to interfacial layer materials, active layer components with state-of-the-art device performance, both polymer and small molecule developed in this laboratory, will also be discussed.

Keywords: polymer solar cell, interfacial layer, self-assembled organic layer, nickel oxide, graphene oxide, zinc oxide, inverted solar cell, organic semiconductor.

1. INTRODUCTION

For solar energy conversion, polymer solar cells (PSCs) have recently attracted great attention as renewable energy sources because of their amenability to fabricating large-area, flexible, and inexpensive devices via low-temperature, high throughput roll-to-roll (R2R) fabrication techniques.¹ Moreover, PSC power conversion efficiencies (PCEs) have increased substantially over past few years and, as a consequence of combined research efforts from synthetic chemists and device engineers, impressive PCEs surpassing 9% have been achieved with PSC active regions configured in a bulk-heterojunction (BHJ) network of interpenetrating π -conjugated polymer electron donors and high electron-affinity fullerene electron acceptors.² PSC performance advances have come mainly from developing new semiconductors for better photon collection and enhanced carrier transport,^{3,4} as well as optimizing materials processing and employing novel device architectures for efficient exciton separation⁵ and photocurrent collection.² Among the various factors determining the PSC performance, the interfacial layers (IFLs) play important roles in organic electronics since charge injection/collection mainly occurs at such interfaces.^{6,7} However, electrode/active layer interfacial phenomena remain understudied in organic optoelectronic device operation, but likely represent a major constraint for breaking the commercialization barrier to achieve 10% PCE and with improved device stability for practical applications.

2. RESULTS AND DISCUSSION

To achieve ohmic contacts for enhancing hole collection and blocking misdirected electrons, poly(3,4-ethylenedioxythiophene):poly(styrene sulfonate) (PEDOT:PSS) is commonly used in BHJ solar cells to optimize the device function, and many examples of promising device performance have been reported usually using PEDOT:PSS as the anode IFL. Nevertheless, as an inhomogeneous aqueous dispersion, PEDOT:PSS is highly hydrophilic and acidic (pH ~1), which can severely degrade device performance during storage by corroding ITO. Furthermore, its structural invariance limits its property modulation, including the energy levels and surface energy. Therefore, the design, synthesis, and incorporation of novel IFLs with tailored optical properties and electronic structures are highly pursued to maximize the device performance and enhance device stability.

This laboratory has been actively engaging in designing novel self-assembled organic interfacial layers for applications in organic light-emitting diodes (OLEDs). The incorporation of such IFLs confines the electron hole recombination in the active layer, rather than at interfaces or electrodes, and dramatically improves OLED efficiency.⁸ Such results for OLED IFLs have profound implications for PSCs since OLEDs and PSCs (or OPVs) have some similarities in function. That is, the operation mechanisms are different but often opposite. By applying what was learned from OLED IFLs, we developed and incorporated novel interfacial layers for polymer solar cell applications, which have impressive charge transporting or blocking characteristics, strong adhesion to anode interface, and great thermal stability.⁹ We first reported a crosslinkable blend of 4,4'-bis[*p*-trichlorosilylpropylphenyl]phenylamino]-biphenyl (TPDSi₂) + poly(9,9-dioctylfluorene-*co*-*N*-[4-(3-methylpropyl)]-diphenylamine) (TFB; Figure 1). The TPDSi₂:TFB films are highly transparent at $\lambda > 400$ nm and can covalently crosslink and bind to the ITO anode after spin-coating. The TPDSi₂:TFB film is homogeneously conductive with a good hole field-effect mobility of 5×10^{-4} cm²/Vs, and a HOMO (-5.3 eV) energetically well-matched with that of the MDMO-PPV blend film HOMO (-5.3 eV, Figure 1) for efficient hole extraction and a high-lying LUMO (-2.3 eV) to block electron leakage to/recombination at, the ITO anode.⁹ The TPDSi₂:TFB IFL is implemented in the well studied MDMO-PPV:PCBM BHJ PSC system. Employing TPDSi₂:TFB as IFL leads to enhanced device performance with $V_{oc} = 0.89$ V, $J_{sc} = 4.62$ mA/cm², $FF = 54.4\%$, and $\eta_p = 2.23\%$ (Figure 2) in comparison to the control devices using PEDOT:PSS as the IFL having $V_{oc} = 0.74$ V, $J_{sc} = 4.56$ mA/cm², $FF = 43.4\%$, and $\eta_p = 1.46\%$. The TPDSi₂:TFB crosslinking ensures that a dense, robust, insoluble, hole-transporting layer is deposited,

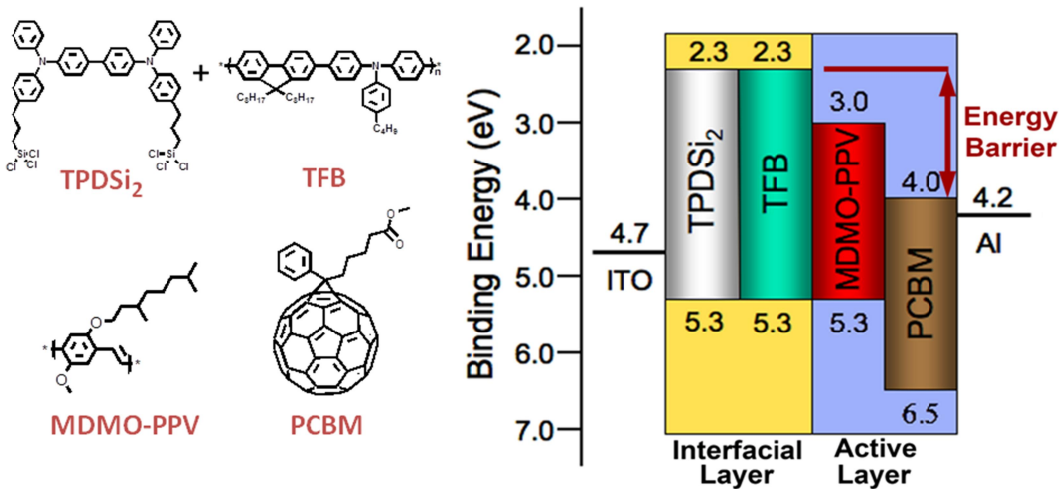


Figure 1. Chemical structures of anode interfacial layer (IFL) components TPDSi₂ and TFB as well as active layer component MDMO-PPV and PCBM and their approximate energy levels.

which can tolerate subsequent active layer solution deposition without dissolving the previously deposited IFL. This organic IFL also has a surface energy comparable to that of the active layer to ensure good wetting, and the covalently bonded IFL is expected to enhance thermal stability. When heated at 60 °C, the TPDSi₂:TFB IFL incorporated polymer solar cells exhibit no significant changes in V_{oc} , J_{sc} , FF , and PCE, in marked contrast to the device performance failure of the control cells with PEDOT:PSS as the IFL.

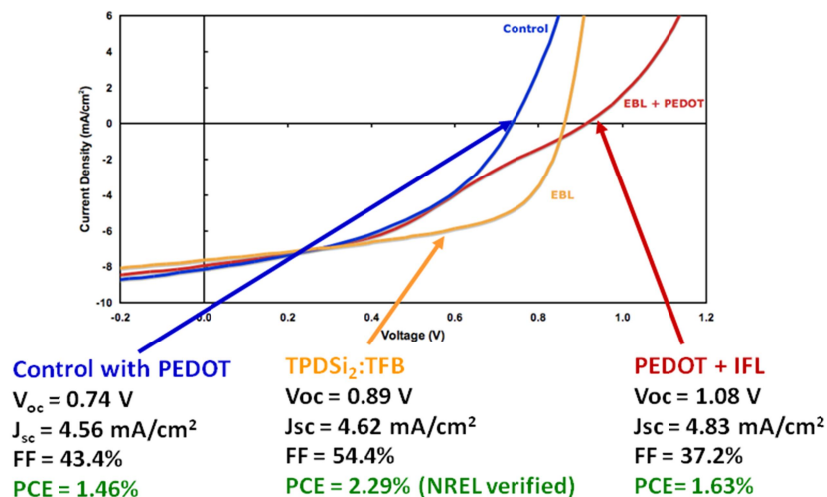


Figure 2. *J-V* curves of MDMO-PPV:PCBM bulk heterojunction polymer solar cells fabricated with PDEOT:PSS, TPDSi₂:TfB, or PEDOT:PSS + TPDSi₂:TfB as an anode interfacial layer.

The effect of ITO anode pre-treatment on the device performance was thoroughly investigated by X-ray photoelectron spectroscopy (XPS) to understand how oxygen plasma, UV ozone, and solvent cleaning greatly affect the device performance in combination without IFL or with different IFLs, such as PEDOT:PSS, TPDSi₂:TfB; PDEO:PSS + TPDSi₂:TfB (Figure 2).¹⁰ O₂ plasma and UV ozone treatment are found to be most effective for creating a hydrophilic surface by removing all organic contaminants when the active layer is to be deposited on a PEDOT:PSS IFL. When using the TPDSi₂:TfB as the IFL, ITO UV ozone treatment produces cells with the optimal performance versus those produced with other cleaning techniques. When active layer is directly deposited on the ITO without any IFL, the cells perform poorly with any ITO treatment because of the very large surface energy mismatch between the ITO anode and the active layers, which exemplifies the importance of using appropriate IFLs in polymer solar cells.

As electron donor layers are varied to advance PSC performance, the interfacial layers must be tailored accordingly in order to obtain the appropriate frontier MO energy matches for ohmic contacts with the active layer and to efficiently block any misdirected charges. In comparison to MDMO-PPV, P3HT shows greatly enhanced PCEs in BHJ polymer solar cells. However the HOMO level of P3HT (-5.0 eV, Figure 3) is significantly higher than that of MDMO-PPV (-5.3 eV), and the TPDSi₂:TfB employed in MDMO-PPV:PCBM cells does not function well when used as the IFL in P3HT:PCBM cells. The energy barrier between TPDSi₂ and P3HT results in an inefficient hole extraction, leading to inferior PCEs with V_{oc} = 0.55 V, J_{sc} = 4.72 mA/cm², FF = 10.4%, and η_p = 0.28%. Thus, 5,5'-bis[(*p*-trichlorosilylpropylphenyl)phenylamino]-2,2'-bithiophene (PABTSi₂; Figure 3) was synthesized, characterized, and

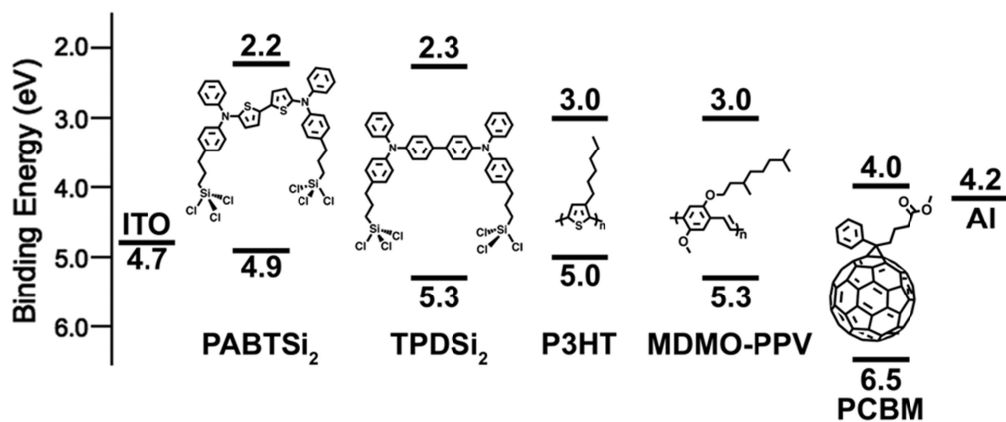


Figure 3. Chemical structures and approximate energy levels of anode interfacial layer components TPDSi₂ and PABTSi₂ as well as active layer component MDMO-PPV, P3HT, and PCBM used in bulk heterojunction polymer solar cells.

implemented as an IFL in P3HT:PCBM polymer solar cells. The PABT_{Si}₂ IFL has well-tuned HOMO energy when employed in P3HT:PCBM PSCs.¹¹ The introduction of electron-rich bithiophene effectively raise the HOMO levels of PABT_{Si}₂ to -4.9 eV and minimize the energy barrier for hole transfer between the active layer and IFL, at the same time, it can effectively block the misdirected electron enabled by its high-lying LUMO level of -2.2 eV. Therefore, the P3HT:PCBM polymer solar cells using PABT_{Si}₂:TFB as IFL afford power conversion efficiency of 3.14% with $V_{oc} = 0.54$ V, $J_{sc} = 9.31$ mA/cm², $FF = 62.7\%$, comparable to those of heavily optimized PEDOT:PSS-based devices.¹¹

NiO, a cubic wide-band gap (3.6 eV) p-type semiconductor, was incorporated into polymer solar cells to facilitate the hole conduction and block electron leakage to ITO.¹² Thin NiO films are essentially transparent for wavelengths > 550 nm (Figure 4a) and its band structure is well-suited for P3HT:PCBM polymer solar cells, and therefore affords an ohmic contact to P3HT (Figure 4b). Thin NiO films were deposited by pulsed-laser deposition (PLD) on ITO anodes, and the presence of crystalline NiO was confirmed by grazing-angle X-ray diffraction. AFM investigation indicates that the NiO deposition significantly planarizes the ITO surface and increases the surface electrical homogeneity.

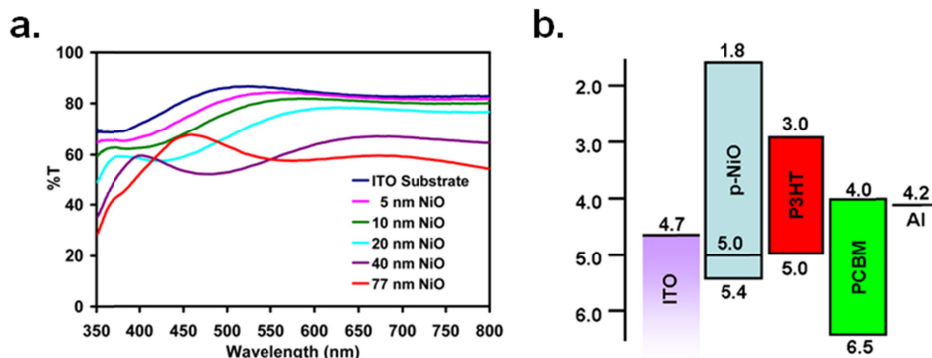


Figure 4. (a) Optical transmission spectra of NiO thin films grown by pulsed-laser deposition having various thicknesses on ITO/glass substrates, the ITO/glass substrate is included as the blank. (b) Energy diagram of device components referenced to the vacuum level, NiO is used as anode interfacial layer. The NiO energy levels are well-situated to block electron leakage to the ITO anode while promoting hole collection.

Device fabrication was first optimized by varying the O₂ partial pressure during NiO film growth and the NiO film thickness. The optimal NiO IFL thickness was found to be 5-10 nm, where an 80% PCE increase is observed versus the control devices (Table 1).¹³ The external quantum efficiency (EQE) for the device containing 10 nm NiO IFL was found to reach a maximum of 87% between 400 and 700 nm, resulting in enhanced J_{sc} . The replacement of PEDOT:PSS with NiO was also found to increase the device open-circuit voltages (V_{oc}) by ca. 0.10 V, which can be attributed to the reduced photocurrent recombination at anodes.¹⁴ The highest PCE from solar cells using NiO as IFL is greater than 5%, and was confirmed by measurements at NREL.

Table 1. Device performance parameters for the glass/ITO/interfacial layer/P3HT:PCBM/LiF/Al bulk heterojunction polymer solar cells.

Device	V_{oc} (V)	J_{sc} (mA/cm ²)	FF (%)	PCE (%)
40 nm PEDOT:PSS	0.583	10.1	64.8	3.81
control	0.515	11.0	50.7	2.87
5 nm NiO	0.634	11.1	63.3	4.45
10 nm NiO	0.638	11.0	69.3	4.88
20 nm NiO	0.591	9.07	55.2	2.96
43 nm NiO	0.586	8.32	52.4	2.55
77 nm NiO	0.581	7.71	49.8	2.23

Grazing incidence wide-angle X-ray scattering (GIWAXS) was used to investigate the morphology of P3HT:PCBM films deposited on NiO and PEDOT:PSS substrates. On the NiO surface, the P3HT adopts a π face-on orientation, in marked contrast to the π edge-on orientation on PEDOT:PSS substrates. The face-on orientation should promote charge migration and extraction, which should enhance PSC J_{sc} s and PCEs using NiO as an IFL. The functionality of NiO IFL in device performance enhancement is further investigated by integrated characterization of the electrical, microstructural, electronic structural, and optical properties of NiO thin films grown on ITO electrodes.¹³ Conductive atomic force microscopy investigations indicate that the NiO thin film can passivate interfacial charge traps. Grazing-incidence X-ray diffraction indicates that the NiO thin films grow preferentially in the (111) directions and to have a fcc NaCl crystal structure.¹³ Diodes of p-n structures and first-principles electronic structure calculations show that the NiO IFL is preferentially conductive to holes. These combined effects result in optimal PSC performance using NiO as an anode IFL.¹³

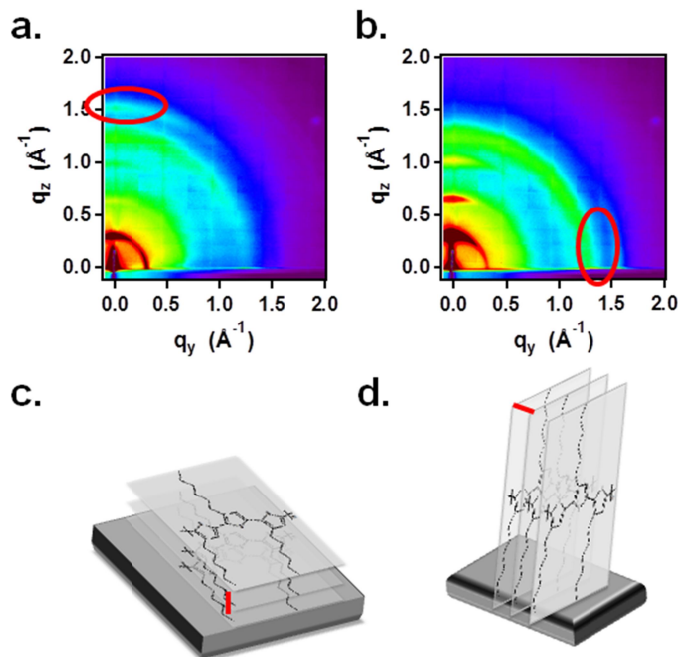


Figure 5. 2D Grazing incidence wide-angle X-ray scattering (GIWAXS) diffraction patterns of P3HT:PCBM film deposited on (a) NiO and (b) on PEDOT:PSS IFL; (c) Schematic diagrams of P3HT π face-on orientation on the NiO IFL and (d) P3HT π edge-on orientation on the PEDOT:PSS IFL.

As the currently most promising polymer semiconductors for solar cell applications, the PTB polymer series³ is receiving great attention from the community for maximum device performance^{2,6} and for fundamental understanding of PSC photophysical processes.¹⁵ GIWAXS studies indicate that the morphologies of seven polymer (PTB1–PTB7) blend films are highly sensitive to the substituents on the two building blocks comprising the polymer backbones, i.e., thienothiophene (TT) and benzodithiophene (BDT).¹⁶ Backbone substituents can greatly affect the polymer backbone π - π stacking in polymer domains and PCBM penetration into these domains. Thus, branched side chain substituents on the BDT units will enlarge the polymer π - π stacking distances and decrease π orbital overlap, and lower the PSC PCEs. However, the branched substituents on the TT units do not interfere with the π - π stacking and can increase the device performance. The PTB polymer series adopts a π face-on orientation on PEDOT:PSS,¹⁶ which is greatly different than the π edge-on orientation of P3HT polymers. Furthermore, there is a positive correlation between polymer π - π stacking distance and solar cell fill factor. As the polymer π - π stacking distance decreases, the fill factor of PTB:PCBM BHJ polymer solar cells increases, which signifies the importance of maximizing the π orbital overlap for increasing charge transport (Figure 6). Additionally, blend films fabricated using processing additives have slightly enhanced polymer crystallinity. Grazing incidence small angle X-ray scattering (GISAXS) studies show that PCBM domains of tens nanometer are present in most BHJ solar cells, but are not present in the PTB-based blend films. The smaller PCBM domain sizes and exceptional penetration into the polymer domain results in interpenetrating bicontinuous network formation, and such film morphologies lead to superior device performance for the PTB series.

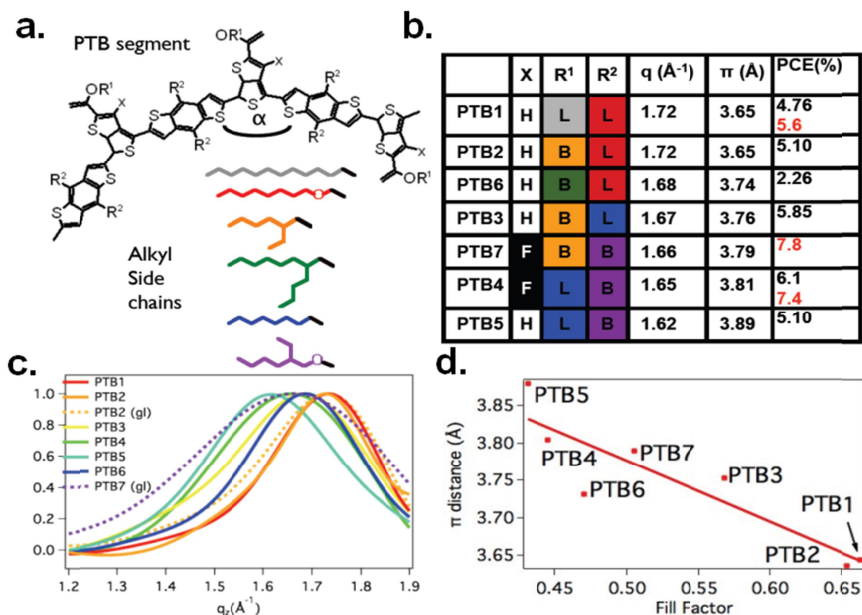


Figure 6. (a) Chemical structures of a PTB polymer series having different substituents on thienothiophene or benzodithiophene units. (b) π - π stacking scattering vectors and linewidths (in parentheses), π - π stacking distances of seven PTB polymer in polymer:PCBM blend film, and the power conversion efficiencies in BHJ polymer solar cells. (c) π - π stacking scattering vector peaks for the PTB series. (d) correlations between polymer π - π stacking distance and the PSC fill factor; the red line is drawn as a visual guide.

Polymer PTB7 shows highly promising device performance in BHJ solar cells, however the incorporation of PEDOT:PSS IFL degrades the PSC performance after device fabrication due to its hydrophilic and acidic characteristics. Graphene oxide (GO) flakes were successfully deposited onto ITO anodes in controlled densities via Langmuir-Blodgett (LB) assembly. The LB-derived GO films achieve good coverage on ITO anode and show greatly reduced film roughness (0.7 nm rms roughness) in comparison to the PEDOT:PSS films (3.5 nm). XPS and Raman spectroscopy confirm that the GO structure remains intact after LB deposition and UV ozone treatment. GIWAX data reveal dominant π face-on orientation of PTB7 on the GO IFL, indicating the GO capability for templating the optimum polymer π -stacking orientation. The BHJ polymer solar cells were next fabricated to investigate the potential of GO as a polymer solar cell IFL, and PCEs up to 7.5% are achieved in the GO-based PSC, which are comparable to the PCEs achieved in PEDOT:PSS-based polymer solar cells. By reducing inhomogeneity-induced recombination processes on the occasionally exposed ITO surfaces, the performance of the LB deposited GO PSCs is expected to be further improved. Furthermore, the GO-based polymer solar cells demonstrate a 5x enhancement in the thermal aging lifetime and a 20x enhancement in humid ambient lifetime in comparison to the PEDOT:PSS-based device analogues. The results indicate great potential of GO as a scalable, substrate-general IFL for high performance and environmentally stable PSCs.

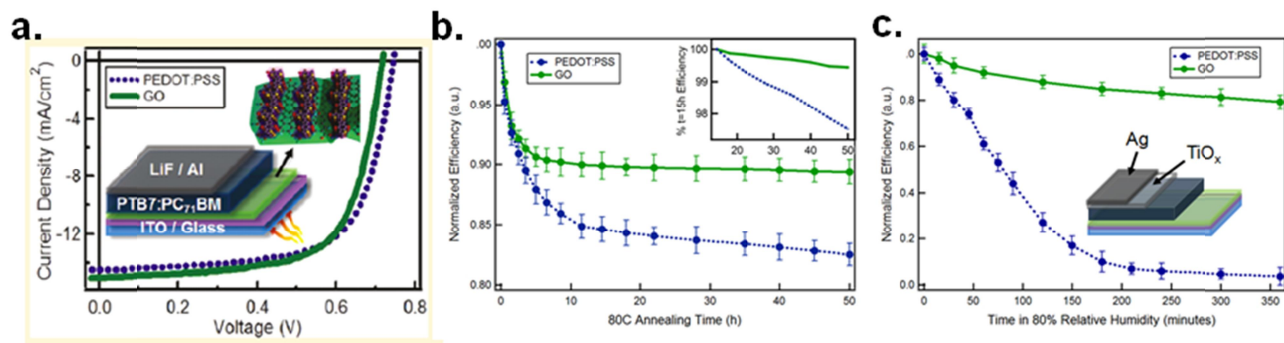


Figure 7. (a) Representative J - V curves for PTB7-based BHJ polymer solar cells fabricated with PEDOT:PSS or GO IFLs; insets show the polymer solar cell structure and preferential PTB7 π face-on orientation on GO/ITO substrates. (b) Thermal degradation of encapsulated polymer solar cells at 80 °C under N_2 ; inset shows data between 15 h and 50 h as a percentage of the efficiency at $t = 15$ h. (c) Environmental degradation of unencapsulated polymer solar cells with Ag cathodes at 80% relative humidity at 25 °C.

In addition to research on IFL engineering, this laboratory is also interested in developing novel high-performance organic semiconductors for PCE enhancement. Useful materials should have broad optical absorption to increase short-circuit currents (J_{sc}) and tailored frontier MOs to maximize the open-circuit voltages (V_{oc}).¹⁷ Organic semiconductors including both small molecules and polymers have their distinctive pros and cons in term of ease of materials synthesis, processing, device fabrication, and performance. In comparison to polymers, small molecules offer great attractions, such as well-defined structures, monodispersity, and minimal batch-to-batch variation in properties. We designed and synthesized a novel building block, the 5,10-bis(2-ethylhexyloxy)naphtho[2,3-b:6,7-b']dithiophene (NDT) moiety. Subsequent coupling with thiophene-capped diketopyrrolopyrrole (TDPP) units affords NDT(TDPP)₂, which shows a promising optical band gap of 1.72 eV and low-lying HOMO energy of -5.40 eV for solar cell applications. Wide-angle X-ray diffraction indicates that NDT(TDPP)₂ achieves long-rang order, confirmed by a substantial hole mobility of $7.18 \times 10^{-3} \text{ cm}^2/\text{Vs}$. BHJ polymer solar cells having device structure of ITO/PEDOT:PSS/-NDT(TDPP)₂:PC₆₁BM/LiF/Al demonstrate excellent device performance with a $V_{oc} = 0.84 \text{ V}$, $J_{sc} = 11.27 \text{ mA}/\text{cm}^2$, $FF = 42\%$, and PCE = 4.06% (Figure 8).¹⁸ The small molecule donor was then further modified, and a “zig-zag” 4,9-bis(2-ethylhexyloxy)naphtho[1,2-b:5,6-b']dithiophene core (zNDT) synthesized and coupled with TDPP to afford the new small molecule semiconductor zNDT(TDPP)₂ (Figure 8),¹⁹ which has an optical band gap very similar to that of NDT(TDPP)₂, but a slightly higher HOMO energy. Interestingly, zNDT(TDPP)₂ achieves higher hole mobilities in both organic thin-film transistors and hole-only diodes in comparison to NDT(TDPP)₂. The higher zNDT(TDPP)₂ hole mobility results in enhanced J_{sc} and FF with slightly smaller V_{oc} in comparison to NDT(TDPP)₂, and therefore a PCE of 4.7% is obtained from zNDT(TDPP)₂:PC₆₁BM PSCs.

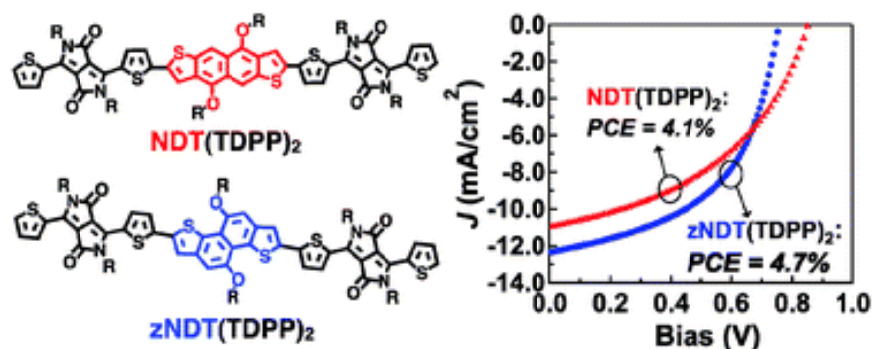


Figure 8. J - V curves of NDT(TDPP)₂ and zNDT(TDPP)₂-based bulk heterojunction polymer solar cells having device structures of ITO/PEDOT:PSS/Donor:PC₆₁BM/LiF/Al

Polymer semiconductors using bithiopheneimides (BTIs) as electron deficient units have also been synthesized for PSCs. The bithiopheneimide unit offers a compact geometry, strong electron-withdrawing character, a planar architecture, and good solubility. Benzodithiophene (BDT) was initially introduced into BTI polymer backbones as electron donor units. The resultant donor-acceptor copolymers have a relatively wide band gap of ca. 1.9 eV (Figure 9), but low-lying HOMOs of -5.50 eV – -5.60 eV, and the derived PSCs achieve V_{oc} s approaching 1.0 V.²⁰ After device optimization,

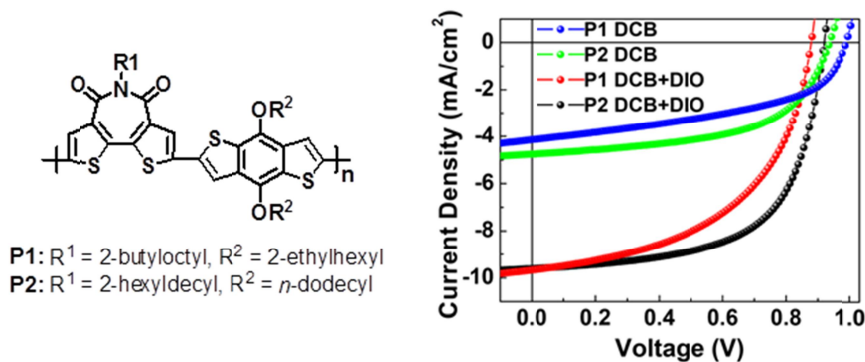


Figure 9. J - V curves of bithiopheneimide-benzodithiophene copolymer-based inverted bulk heterojunction PSCs having the device structures ITO/ZnO/polymer:PC₇₁BM/MoO_x/Ag.

inverted solar cells having the structure ITO/ZnO/polymer:PC₇₁BM/MoO_x/Ag, in which the ZnO cathode IFL is prepared by sol-gel techniques, exhibit promising PCEs up to 5.5%, mainly due to the large V_{oc} s. The inverted device architecture eliminates the use of PEDOT:PSS as the anode IFL, and therefore the cells show improved device air stability.²⁰

Bithiopheneimide-benzodithiophene copolymer solar cell performance is mainly limited by the large band gaps due to unfavorable BDT unit quinoidal character, which limits exciton formation. As widely used electron-rich co-units, dithienosilole (DTS) or dithienogermole (DTG) were then incorporated into the polymer backbones, and the resultant polymer semiconductors PBTiSi and PBTiGe show lower band gaps of 1.73 – 1.75 eV, with low-lying HOMO energies of ca. -5.40 eV.²¹ After optimization, inverted polymer solar cells having device structures ITO/ZnO/polymer:PC₇₁BM/MoO_x/Ag achieve PCEs greater than 6.4% (Figure 9). A film morphology investigation indicates that these polymers have a very close π - π stacking distance of 3.5 Å, and adopt a π face-on orientation on the ZnO IFL, which should benefit charge extraction, in good agreement with the PSC performance.²¹

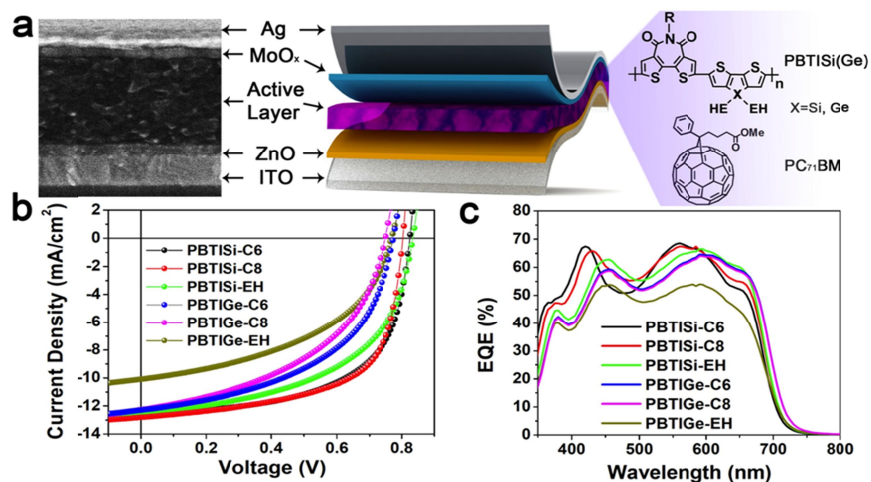


Figure 10. Inverted PSC device structure and performance of bithiopheneimide-dithienosilole (PBTiSi) or bithiopheneimide-dithienogermole (PBTiGe) copolymers having different substituents: (a) SEM cross-sectional image of a PBTiSi-C8:PC₇₁BM (1:1) device fabricated with DCB:DIO (98:2 v/v) as the processing solvent; (b) J - V curves of optimized PBTiSi and PBTiGe-based PSCs; (c) External quantum efficiencies of the best performing solar cells.

Next, using bithiopheneimides as acceptor units, recently developed crystalline polymer semiconductors achieve PCEs up to 8.6% with unprecedented FF s of 76–80% in inverted polymer solar cells.²² Film morphology and microstructure investigations show that the blend polymer films achieve optimal horizontal and vertical phase gradation on the ZnO IFL. S and C mapping of the active layer cross-sections by energy-dispersive X-ray spectroscopy (EDS) and depth-

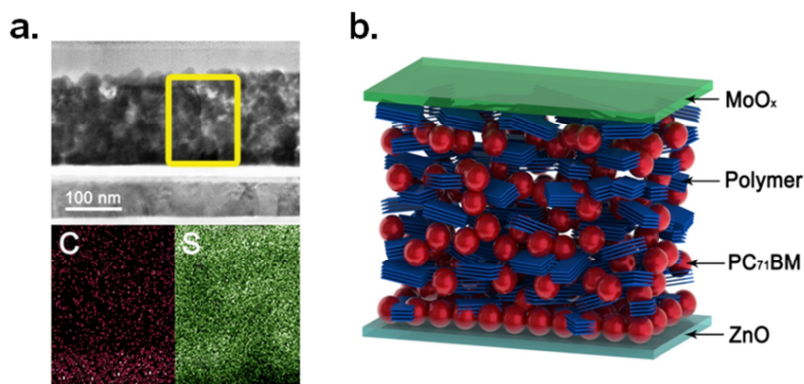


Figure 11. (a) EDS carbon and sulfur mappings of an optimized bithiopheneimide polymer-based inverted solar cell, in which a PC₇₁BM-rich domain forms at the blend/ZnO interface. (b) Schematic diagram of the polymer:PC₇₁BM blend film, showing vertical phase gradation with a polymer-rich layer near the MoO_x/blend interface and a PC₇₁BM-rich layer near the blend/ZnO interface.

profiled XPS (Figure 11), reveals a C-rich layer at the blend/ZnO interface, distinct from the bulk film. Correspondingly, the S content at this interface is significantly depleted, indicating PC₇₁BM enrichment near the blend/ZnO interface.²² These results indicate that the using ZnO as IFL in combination with inverted device architecture should be an effective strategy for increasing the device performance of polymer solar cells due to the desired vertical phase gradation induced by the surface energy difference between polymer and PC₇₁BM, and their interactions with ZnO IFL.

3. CONCLUSIONS

A variety of interfacial layers with well-tuned optical properties and electronic structures have been designed, synthesized, and incorporated into bulk heterojunction PSCs. The interfacial layers include self-assembled organic materials, metal oxide films, and emerging materials, such as graphene oxide. The organic self-assembled layers can crosslink to form homogeneous, transparent, and robust layers on the ITO anodes, allowing subsequent solution-deposition of the active layers. The resultant polymer solar cells achieve device performance comparable or superior to conventional solar cells using PEDOT:PSS as the IFL, but having enhanced device air-stability. The new IFL anode coatings can be tuned for orbital energetic matching with various active layer components. The metal oxides, NiO and ZnO, show great potential for application in PSCs. The p-type NiO, when used as the hole transporting/electron blocking layer, results in dramatically enhanced performance of P3HT/PCBM polymer solar cells with PCE up to 5%. Using ZnO as electron transporting/hole blocking layer, inverted PSCs achieve desired donor molecule π -orientation and vertical phase separation, and therefore extremely high fill factors and PCEs. Graphene oxide (GO) is also successfully employed as a PSC IFL, and the Langmuir-Blodgett derived GO-based solar cells achieve PCE of 7.5%, but with enhanced device air-stability. The results indicate the great potentials of GO as scalable, substrate-general IFL for high performance and environmentally stable PSCs. In addition to IFLs, state-of-the-art electron donor materials have also been reported, both small molecules and polymers, and BHJ polymer systems exhibit power conversion efficiencies greater than 8%.

4. ACKNOWLEDGMENTS

This research is supported by the ANSER Center, an Energy Frontier Research Center funded by the U.S. Department of Energy, Office of Science, and Office of Basic Energy Sciences under Award Number DE-SC0001059 (organic IFLs and polymer photovoltaics), by the Department of Energy Basic Energy Sciences under Award No. DE-FG02-08ER46536 (inorganic IFLs), and by the Air Force Office of Scientific Research under grant FA9550-08-1-0331 (polymer semiconductors and transistors).

5. REFERENCES

- [1] Service, R. F., "Outlook brightens for plastic solar cells," *Science*, 332, 293-293 (2011).
- [2] He, Z., Zhong, C., Su, S., Xu, M., Wu, H. and Cao, Y., "Enhanced power-conversion efficiency in polymer solar cells using an inverted device structure," *Nat. Photonics*, 6(9), 591-595 (2012).
- [3] Liang, Y. and Yu, L., "A new class of semiconducting polymers for bulk heterojunction solar cells with exceptionally high performance," *Acc. Chem. Res.* 43(9), 1227-1236 (2010).
- [4] Boudreault, P.-L. T., Najari, A. and Leclerc, M., "Processable low-bandgap polymers for photovoltaic applications," *Chem. Mater.* 23(6), 456-469 (2011).
- [5] Peet, J., Heeger, A. J. and Bazan, G. C., "'Plastic' solar cells: self-assembly of bulk heterojunction nanomaterials by spontaneous phase separation," *Acc. Chem. Res.* 42(11), 1700-1708 (2009).
- [6] He, Z., Zhong, C., Huang, X., Wong, W.-Y., Wu, H., Chen, L., Su, S. and Cao, Y., "Simultaneous enhancement of open-circuit voltage, short-circuit current density, and fill factor in polymer solar cells," *Adv. Mater.* 23(40), 4636-4643 (2011).
- [7] Amb, C. M., Chen, S., Graham, K. R., Subbiah, J., Small, C. E., So, F. and Reynolds, J. R., "Dithienogermole as a fused electron donor in bulk heterojunction solar cells," *J. Am. Chem. Soc.* 133(26), 10062-10065 (2011).
- [8] Yan, H., Lee, P., Armstrong, N. R., Graham, A., Evmenenko, G. A., Dutta, P. and Marks, T. J., "High-performance hole-transport layers for polymer light-emitting diodes. Implementation of organosiloxane cross-linking chemistry in polymeric electroluminescent devices," *J. Am. Chem. Soc.* 127 (9), 3172-3183 (2005).
- [9] Hains, A. W. and Marks, T. J., "High-efficiency hole extraction/electron-blocking layer to replace poly(3,4-ethylenedioxythiophene):poly(styrene sulfonate) in bulk-heterojunction polymer solar cells," *Appl. Phys. Lett.* 92(2), 023504 (2008).

- [10] Hains, A. W., Liu, J., Martinson, A. B. F., Irwin, M. D. and Marks, T. J., "Anode interfacial tuning via electron-blocking/hole-transport layers and indium tin oxide surface treatment in bulk-heterojunction organic photovoltaic cells," *Adv. Funct. Mater.* 20(4), 595-606 (2010).
- [11] Hains, A. W., Ramanan, C., Irwin, M. D., Liu, J., Wasielewski, M. R. and Marks, T. J., "Designed bithiophene-based interfacial layer for high-efficiency bulk-heterojunction organic photovoltaic cells. Importance of interfacial energy level matching," *ACS Appl. Mater. Interfaces* 2(1), 175-185 (2010).
- [12] Irwin, M. D., Buchholz, D. B., Hains, A. W., Chang, R. P. H. and Marks, T. J., "p-Type semiconducting nickel oxide as an efficiency-enhancing anode interfacial layer in polymer bulk-heterojunction solar cells," *Proc. Natl. Acad. Sci. U.S.A.* 105(8), 2783-2787 (2008).
- [13] Irwin, M. D., Servaites, J. D., Buchholz, D. B., Leever, B. J., Liu, J., Emery, J. D., Zhang, M., Song, J.-H., Durstock, M. F., Freeman, A. J., Bedzyk, M. J., Hersam, M. C., Chang, R. P. H., Ratner, M. A. and Marks, T. J., "Structural and electrical functionality of NiO interfacial films in bulk heterojunction organic solar cells," *Chem. Mater.* 23(8), 2218-2226 (2011).
- [14] Steirer, K. X., Chesin, J. P., Widjonarko, N. E., Berry, J. J., Miedaner, A., Ginley, D. S. and Olson, D. C., "Solution deposited NiO thin-films as hole transport layers in organic photovoltaics," *Org. Electron.* 11(8), 1414-1418 (2010).
- [15] Rolczynski, B. S., Szarko, J. M., Son, H. J., Liang, Y., Yu, L. and Chen, L. X., "Ultrafast intramolecular exciton splitting dynamics in isolated low-band-gap polymers and their implications in photovoltaic materials design," *J. Am. Chem. Soc.* 134(9), 4142-4152 (2012).
- [16] Szarko, J. M., Guo, J., Liang, Y., Lee, B., Rolczynski, B. S., Strzalka, J., Xu, T., Loser, S., Marks, T. J., Yu, L. and Chen, L. X., "When function follows form: effects of donor copolymer side chains on film morphology and BHJ solar cell performance," *Adv. Mater.* 22(48), 5468-5472 (2010).
- [17] Cheng, Y.-J., Yang, S.-H. and Hsu, C.-S., "Synthesis of conjugated polymers for organic solar cell applications," *Chem. Rev.* 109(11), 5868-5923 (2009).
- [18] Loser, S., Bruns, C. J., Miyauchi, H., Ortiz, R. P., Facchetti, A., Stupp, S. I. and Marks, T. J., "A naphthodithiophene-diketopyrrolopyrrole donor molecule for efficient solution-processed solar cells," *J. Am. Chem. Soc.* 133(21), 8142-8145 (2011).
- [19] Loser, S., Miyauchi, H., Hennek, J. W., Smith, J., Huang, C., Facchetti, A. and Marks, T. J., "A "zig-zag" naphthodithiophene core for increased efficiency in solution-processed small molecule solar cells," *Chem. Commun.* 48(68), 8511-8513 (2012).
- [20] Zhou, N., Guo, X., Ortiz, R. P., Li, S., Zhang, S., Chang, R. P. H., Facchetti, A. and Marks, T. J., "Bithiophene imide and benzodithiophene copolymers for efficient inverted polymer solar cells," *Adv. Mater.* 24(7), 2242-2248 (2012).
- [21] Guo, X., Zhou, N., Lou, S. J., Hennek, J. W., Ortiz, R. P., Butler, M. R., Boudreault, P.-L. T., Strzalka, J., Morin, P.-O., Leclerc, M., López Navarrete, J. T., Ratner, M. A., Chen, L. X., Chang, R. P. H., Facchetti, A. and Marks, T. J., "Bithiopheneimide-dithienosilole/ithienogermole copolymers for efficient solar cells: information from structure-property-device performance correlations and comparison to thieno[3,4-c]pyrrole-4,6-dione analogues," *J. Am. Chem. Soc.* 134(44), 18427-18439 (2012).
- [22] Guo, X., Zhou, N., Lou, S. J., Hennek, J. W., Ortiz, R. P., Strzalka, J., Chen, L. X., Chang, R. P. H., Facchetti, A. and Marks, T. J., "unpublished results."